Keywords
INOX; Nanoksa G-Plus; scaffold; periodontal regeneration; peri-implant tissue engineering; cytocompatibility; osteogenic differentiation; fibroblasts; ALP; RUNX2; osteocalcin; MTT assay; DNA integrity; high-performance polymer

Authors -
Ghada Gamal Adayil[1*]
BDS, M.Sc, PhD; Lecturer of Periodontology, Department of Oral Medicine and Periodontology, Faculty of Dentistry, Cairo University, Email: Ghada.adayil@dentistry.cu.edu.eg
ORCID: 0009-0007-0022-1558

Mihad Ibrahim[2]
BDS, M.Sc, PhD candidate, Department of Periodontology, Faculty of Dentistry, Cairo University, Email: mihad.ibrahim@dentistry.cu.edu.eg
ORCID: 0009-0003-2127-9442

Hazem Ahmed Elsayed[3]
BDS, M.Sc candidate, Department of Periodontology, Faculty of Dentistry, Cairo University, Email: hazem.elsayed@dentistry.cu.edu.eg
ORCID: 0009-0001-4123-0238

Marwa A. El-Saeed[4]
BDS, M.Sc, PhD, Lecturer of Oral Biology, Department of Oral Biology, Faculty of Dentistry, Cairo University, Email: marwa.elsaeed@dentistry.cu.edu.eg
ORCID:0000-0002-9090-2352

Received: 05.03.2026
Revised: 25.03.2026
Accepted: 29.04.2026
Doi:10.1922/ejprd.v34i3s.1391

Cytotoxicity Evaluation of INOX (Nanoksa G Plus) High-Performance Polymer Discs on Cell Cultures: An In-Vitro Experimental Study

ABSTRACT

Background/Objectives: INOX (Nanoksa G-Plus) is a nano-reinforced high-performance polymer composed of a methacrylate-based matrix reinforced with nano-zirconia and nano-carbon fillers, currently used as a CAD/CAM restorative material for full-arch implant-supported frameworks and denture bases. Despite its increasing clinical use, comprehensive biological characterization, particularly its potential to support regenerative cellular responses, remains unexplored. The present study aimed to evaluate the cytocompatibility, osteogenic differentiation potential, and genotoxic profile of INOX in human fibroblasts, to establish its candidacy as a scaffold material for periodontal and peri-implant regeneration.

Methods: Human skin fibroblast cells (HFB4); VACSERA, Cairo, Egypt, were exposed to two-fold serial dilutions of INOX extract 1500–0.73 µg/mL. Cytocompatibility was assessed using the MTT colorimetric viability assay ISO 10993-5. Osteogenic gene expression was quantified by real-time quantitative polymerase chain reaction (RT-qPCR) targeting alkaline phosphatase (ALP), runt-related transcription factor 2 (RUNX2), and osteocalcin (OCN). DNA integrity was assessed by the diphenylamine (DPA) colorimetric assay and confirmed by agarose gel electrophoresis. Surface characteristics of the material and fibroblast morphology were further examined using scanning electron microscopy (SEM).

Results: Cell viability ranged from 82.62% to 101.59% across all tested concentrations, consistently exceeding the 70% ISO 10993-5 non-cytotoxicity threshold. RT-qPCR revealed significant upregulation of ALP fold change: 2.96, RUNX2 fold change: 2.18, and OCN fold change: 3.18 in INOX-exposed fibroblasts relative to untreated controls. DNA fragmentation was minimal and comparable between groups: test: 2.14 ± 0.08%; control: 1.80 ± 0.05%, with agarose gel electrophoresis confirming predominant genomic integrity in both groups.

Table 4: Percent DNA fragmentation and corresponding optical density OD values in

	% DNA	Optical density								
	fragmentation	S	ΔT	ΔB	T1	T2	T3	B1	B2	B3
INTRODUC	S/HFB4	2.144559		0.018	0.821333	0.022	0.017	0.015	0.823	0.819	0.822
	C/HFB4	1.800327		0.014667	0.8	0.015	0.013	0.016	0.792	0.802	0.806

HFB4 cells for the test compound S and control C. T1–T3 represent test sample readings, B1–B3

Conclusions: INOX demonstrates robust cytocompatibility and the capacity to stimulate osteogenic differentiation markers in fibroblasts without inducing genotoxic damage. These findings support the translational potential of INOX as a bioactive scaffold platform for periodontal regeneration and peri-implant tissue engineering, bridging its established role as a prosthetic framework material with a novel regenerative function.

1. INTRODUCTION

Periodontal disease and peri-implant soft and hard tissue defects are two of the most widespread and difficult-to-treat conditions in modern dentistry [1]. Periodontitis, which affects 45-50% of the world's adult population, results in irreversible deterioration of the periodontal apparatus of the tooth, including the periodontal ligament (PDL), alveolar bone and cementum [2]. Peri-implantitis, an infectious-inflammatory disease of the soft and hard tissues around osseointegrated implants, is similarly destructive in nature and may occur in up to 22% of patients [3]. These two conditions require regenerative approaches that have the potential to regenerate lost tissue architecture and guarantee long-term functional and biological integration [4].

The area of tissue engineering and regenerative medicine has revolutionized the clinical treatment of periodontal and peri-implant defects [4]. The classical triad of regeneration cells, signals and scaffolds has led studies during the last three decades [5]. The scaffold has a central place in these components: it gives the three-dimensional architectural template guiding cell adhesion, proliferation and differentiation as well as allowing tissue ingrowth and providing cellular microenvironmental regulation cues to the local cellular environment [5,6]. The ideal scaffold in periodontal applications should possess the following characteristics; adequate mechanical properties, surface biocompatibility, osteogenic and fibroblastic differentiation and stability to meet the dynamic loading conditions in the oral cavity [7].

High-performance polymers -HPPs- have become an attractive group of scaffold prospects because of their good modulus of elasticity, biocompatibility, and computer-aided design and computer-aided manufacturing (CAD/CAM) manufacturability [8]. The most researched HPP in the dental field, polyetheretherketone (PEEK), has been shown to exhibit bone-like elasticity, chemical inertness, and biocompatibility, which make it useful in abutments of implants, endosseous implants, and regenerative membranes [9]. Nonetheless, the bioinertness of unmodified PEEK, which is a hydrophobic surface with low protein adsorption and cell attachment, is a primary drawback of the material in tissue engineering applications [10]. Various modifications such as roughening of the surfaces, plasma treatment and bioactive filler inclusion have been investigated to address these limitations [10,11].

In spite of such benefits, PEEK has drawbacks. It is very expensive and can only be used in the demanding clinical cases and processing requires special and high temperature equipment as well as specialized technique. The material can be degraded under the influence of strong oxidising acids, including sulfuric, nitric, and chromic acids, and halogen and its resistance to ultraviolet is limited [12]. These limitations should be taken into account when choosing PEEK as a periodontal and implant material, yet when used properly, it promises to be an alternative that could be used to improve the preservation of both hard and soft tissues.

INOX (Nanoksa G-Plus; B&E Bio-Technology Co., Ltd., Seoul, Republic of Korea) is a novel generation HPP developed from a methacrylate-based polymer matrix reinforced with nano-zirconia and nano-carbon fillers [13]. It is currently indicated for the fabrication of full-arch implant-supported prosthetic frameworks, denture bases, and multi-unit restorations, where it has demonstrated favorable mechanical performance, including high flexural strength, wear resistance, and dimensional stability under simulated intraoral conditions [14]. Its nano-reinforced composite structure may confer surface properties, including micro-scale roughness arising from nano-filler distribution, that are conducive to protein adsorption, cell attachment, and downstream cellular differentiation, properties critically important in a scaffold context [14].

Fibroblasts are among the most biologically and clinically relevant cell populations to consider in the context of periodontal and peri-implant regeneration [15]. Periodontal ligament fibroblasts (PDLFs) are the dominant cell type of the periodontal ligament and are recognized as having unique multipotent properties, including the capacity to express osteogenic markers such as alkaline phosphatase (ALP), runt-related transcription factor 2 (RUNX2), and osteocalcin (OCN), and to contribute to both cementogenesis and alveolar bone formation under appropriate stimulatory conditions [16]. Gingival fibroblasts similarly play a critical role in peri-implant soft tissue integration and wound healing [17]. The use of fibroblast cell lines in preliminary scaffold biocompatibility assessments provides a biologically meaningful and internationally accepted model for evaluating both cytotoxic potential and the capacity to stimulate pro-regenerative gene expression [18].

Despite the growing clinical deployment of INOX in implant prosthetics, no published study has systematically evaluated its biological safety at the cellular level, nor has its capacity to support osteogenic signaling been investigated. This gap is particularly significant given the increasing recognition that restorative materials in contact with peri-implant tissues

must not merely be bioinert but may ideally stimulate tissue integration and regeneration. The current research was aimed to fill this gap by performing a full in vitro biological characterization of INOX with human fibroblast cells.

In particular, the study intended to: determine the cytocompatibility of INOX under various concentrations, measure the osteogenic gene expression response of fibroblasts subjected to INOX extract, and assess the genotoxic potential of the material to present a holistic biological profile of INOX, with direct implications to its possible application as a regenerative scaffold in periodontology and implant dentistry.

2. MATERIALS AND METHODS

2.1. Study Design

This in vitro experimental laboratory study was designed as a controlled clinical trial of the biological response of human fibroblast cells to INOX (Nanoksa G-Plus- extract). The experimental protocol was reviewed and approved by the Research Ethics Committee (REC) of the Faculty of Dentistry, Cairo University -Approval No. 35-10-25-. Cytotoxicity testing was conducted in accordance with ISO 10993-5 -2009- [19] for the in vitro biological evaluation of medical devices. No human participants or animal subjects were involved in this study, and all procedures were carried out using commercially sourced cell lines under standard laboratory conditions.

Because this study was designed as a preliminary in vitro biological evaluation, no formal a priori sample size calculation was performed. Experimental replication was based on standard practice for cell culture biomaterial assays, and all measurements were obtained from independent replicates with technical repetition where applicable.

2.2. Test Material

INOX (Nanoksa G-Plus; B&E Bio-Technology Co., Ltd., Seoul, Republic of Korea) is a nano-reinforced high-performance polymer disc system composed of a methacrylate-based polymer matrix incorporating nano-zirconia and nano-carbon fillers. It is manufactured via CAD/CAM milling technology and is indicated for the fabrication of implant-supported full-arch frameworks, denture bases, and multi-unit prosthetic restorations. Specimens of INOX (Nanoksa G-Plus) were fabricated from commercially available CAD/CAM discs using a computer-aided milling system. Cylindrical discs measuring 10 mm in diameter and 2.5 mm in thickness were prepared. Milling was performed using a 5-axis CAD/CAM milling unit -Ceramill Motion 2 Hybrid; Amann Girrbach, Austria- operating in wet/dry hybrid mode. The discs were mounted in a 98-mm CAD/CAM disc holder -Blank Holder 98 M2; Amann Girrbach- during the milling process.

Following milling, specimens were cleaned with isopropanol to remove surface contaminants and debris generated during the machining process and allowed to air-dry under sterile conditions before further experimental procedures.

2.3. Cell Culture

The “Egyptian Holding Company on Biological Products and Vaccines” (VACSERA), Cairo, Egypt- acquired “human skin fibroblast cells” (HFB4) and were cultured under normal conditions at 37oC in the presence of 5% CO2 and humidity. The cells were cultured in complete RPMI-1640 medium with 10% fetal bovine serum (FBS) and 1% penicillin-streptomycin. In case of experimental assays, cells were seeded in 96-well microtiter plates with 1 × 105 cells/mL and left to adhere after 24 hours of treatment. Figure 1 shows the work flow of the experimental methodology.

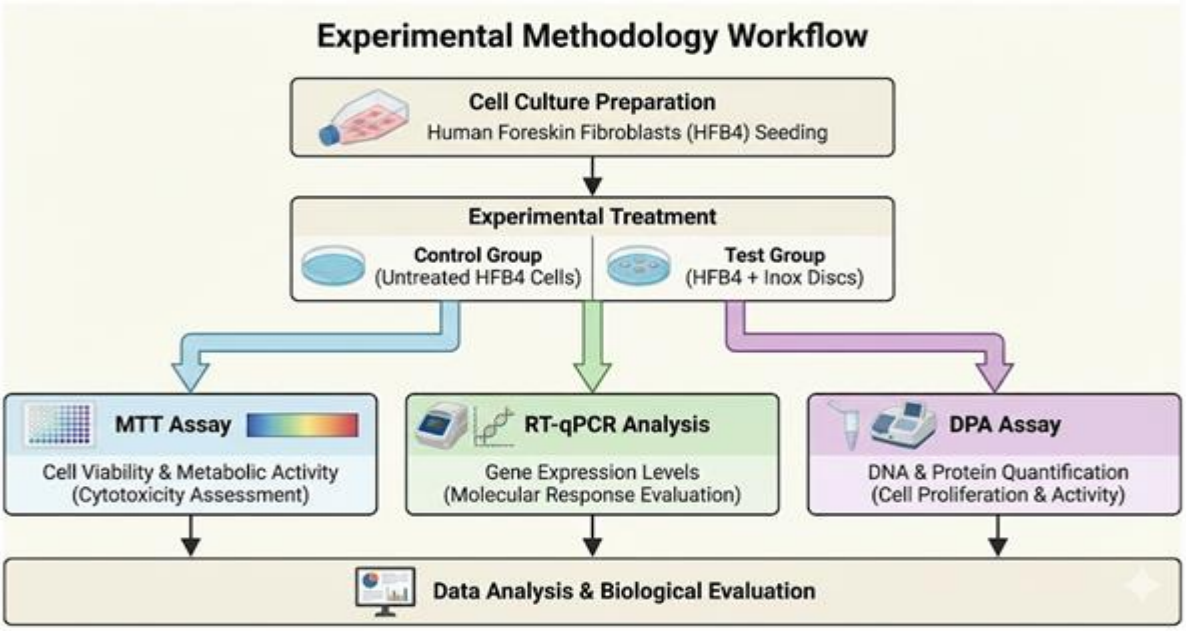

Figure 1. Schematic illustration of the experimental methodology workflow.

2.4. Preparation of INOX Extract and Treatment Concentrations:

INOX extract was prepared by immersing standardized specimens of known surface area in complete cell culture medium at 37 °C for 24 hours in a 5% CO_2 atmosphere, following the extract preparation principles outlined in ISO 10993-12 [20]. The resulting eluate was filter-sterilized through a 0.22-µm membrane filter and used as the stock extract concentration. Cells were exposed to two-fold serial dilutions beginning at a starting concentration of 1500 µg/mL, proceeding through 750, 375, 187.5, 93.75, 46.88, 23.44, 11.72, 5.86, 2.93, 1.46, and 0.73 µg/mL, yielding twelve concentration steps. Untreated cells receiving fresh medium alone served as the negative (vehicle) control.

2.5. MTT Cell Viability Assay

Cytotoxicity was assessed using the "3-4,5-dimethylthiazol-2-yl-(2,5-diphenyltetrazolium bromide) (MTT) assay" as previously described [21].The culture medium was aspirated and replaced with 200 µL of INOX extract at each serial dilution following a 24-hour attachment period, prepared as described above. Treated plates were incubated at 37 °C for 24 hours. After the exposure period, plates were examined under an inverted light microscope for morphological assessment and to confirm the absence of microbial contamination. Dead and detached cells were removed by washing with "phosphate-buffered saline" (PBS; pH 7.2 ± 0.2, 0.05% Tween). Each well was incubated with MTT solution -0.5% (25 µL/well), and the plates were then incubated at 37oC to allow the formation of intracellular formazan crystals (3 -4 hours). To dissolve the formazan crystals, 50 µL "dimethyl sulfoxide" (DMSO) was added to each of the wells, and incubated on a plate shaker over 30 minutes. "Optical density" (OD) was measured at 570 nm using an "ELISA microplate reader" (Biotek 800, USA). All experiments were performed in triplicate. The half-maximal inhibitory concentration (IC_{50}) was calculated using MasterPlex 2010 software. Cell viability percentage was calculated as:

Cell viability (%) = [OD of treated cells / OD of untreated control cells] × 100

Materials exhibiting ≥70% cell viability were classified as non-cytotoxic in accordance with ISO 10993-5 criteria.

2.6. RT-qPCR Analysis of Osteogenic Gene Expression

2.6.1. RNA Extraction

HFB4 fibroblast cells were divided into two experimental groups: INOX-treated cells (S/HFB4) and untreated control cells (C/HFB4). All RNA extraction procedures were conducted under strictly RNase-free conditions. Work surfaces and the homogenizer were decontaminated with RNaseZap, bleach, and 70% ethanol before use. Frozen cell pellets were retrieved from −80 °C storage and maintained on dry ice. Total RNA was extracted using TRIzol reagent -1 mL per sample- following homogenization for 60 seconds. Following a 5-minute room-temperature incubation, chloroform -200 µL per 1 mL TRIzol- was added, vortexed vigorously for 15 seconds, and incubated for a further 2–3 minutes. Samples were centrifuged at 12,000 × g for 15 minutes at 4 °C to achieve phase separation. The aqueous phase containing RNA on the top was gently spun without disturbing the interphase and placed in a clean tube. An equal volume of 70% ethanol was put in, and the mixture was applied to an RNeasy Mini Kit column (Qiagen). Columns were centrifuged in series and washed in RW1 and RPE buffers and DNase I was applied on-column to eliminate any residual genomic DNA. RNA was eluted with 30 µL of RNase-free water. RNA quantity and purity were assessed spectrophotometrically using a NanoDrop system, with acceptable thresholds defined as an A260/A280 ratio of approximately 1.9–2.1 and an A260/A230 ratio >2.0. RNA integrity was verified with 1% agarose gel electrophoresis or Bioanalyzer analysis (RIN >8).

2.6.2. cDNA Synthesis

The reverse-transcription of complementary DNA (cDNA) was performed on 1 µg of total RNA per sample using the High-Capacity cDNA Reverse Transcription Kit (Applied Biosystems, Thermo Fisher Scientific, USA) in a final volume of 20 µL. The reverse transcription protocol was the following cycling conditions: 25 °C for 10 minutes -primer annealing-, 37 °C for 120 minutes (cDNA synthesis), and 85 °C for 5 minutes enzyme inactivation. qPCR was performed on the resultant cDNA diluted in nuclease-free water.

Sample	1	2	3	4	5	6	7	8	9	10	11	12
Test group	0.35	0.373	0.407	0.372	0.392	0.381	0.386	0.392	0.374	0.421	0.429	0.422
	0.342	0.368	0.349	0.365	0.361	0.385	0.372	0.394	0.424	0.421	0.424	0.432
	0.349	0.346	0.338	0.364	0.357	0.373	0.389	0.383	0.435	0.43	0.42	0.426

Average	0.35	0.36	0.36	0.37	0.37	0.38	0.38	0.39	0.41	0.42	0.42	0.43
Viability%	82.62	86.27	86.83	87.38	88.10	90.40	91.03	92.78	97.86	100.95	101.03	101.59
Cell control	0.373	0.446	0.373	0.421	0.389	0.421	0.452	0.444	0.41	0.389	0.373	0.452
	0.452	0.389	0.421	0.452	0.41	0.434	0.421	0.399	0.452	0.421	0.369	0.41
Average	0.41	0.42	0.40	0.44	0.40	0.43	0.44	0.42	0.43	0.41	0.37	0.43
Average of all cell control	**0.42**											

Table 1: MTT assay results showing optical density readings, averaged values, and calculated cell viability percentages % for the test group compared to the cell control.

2.6.3. Quantitative PCR

The quantitative PCR was done with SYBR Green master mix (Bio-Rad Laboratories, USA) in Rotor-Gene 6000 real-time PCR system (Corbett Research, Australia). "Alkaline phosphatase" (ALP), "runt-related transcription factor 2" (RUNX2), and "osteocalcin" (OCN) were used as target genes and "glyceraldehyde-3-phosphatase dehydrogenase" (GAPDH) was the endogenous reference housekeeping gene. The sequences of the primers in this study are provided in Supplementary Table 1. Exon exon junction primers were designed to span exons to eliminate genomic DNA amplification, and all pairs were tested to amplify efficiently (90-110%) and selectively (single melt-curve peak).

Each 20 µL qPCR reaction contained SYBR Green master mix, gene-specific forward and reverse primers at a final concentration of 300 nM each, cDNA template, and nuclease-free water. Thermal cycling conditions were as follows: initial UDG activation at 50 °C for 2 minutes; polymerase hot-start activation at 95 °C for 2 minutes; followed by 40 cycles of denaturation at 95 °C for 15 seconds and combined annealing/extension at 60 °C for 1 minute. Melt-curve analysis was performed at the end of amplification to confirm product specificity. All reactions were performed in triplicate. Relative gene expression was calculated using the comparative 2

Relative gene expression was calculated using the comparative $2^{-\Delta\Delta Ct}$ method. Ct values of each target gene were normalized to the GAPDH reference -ΔCt-, and ΔΔCt was calculated as the difference between treated and control ΔCt values. Fold changes in expression are reported as $2^{-\Delta\Delta Ct}$. Statistical significance was defined as $p < 0.05$.

2.7. DNA Fragmentation Analysis -DPA Assay-

The DNA integrity was determined by the diphenylamine (DPA) colorimetric assay, which is based on the fact that, when DNA is highly fragmented, a large part of the longer strands of DNA can be centrifugally sedimented, and the remaining intact DNA can be centrifugally recovered as chromosomes. Briefly, 1 mL of cell suspension -1–5 × 10^6 cells/mL in complete RPMI (1640) was centrifuged at 200 × g for 10 minutes at 4 °C. Part of the supernatant fraction -S- was transferred to a labeled tube. The cell pellet -B- was washed in 1 mL of TTE solution -TE buffer, pH 7.4, with 0.2% Triton X-100- and vortexed forcefully to lysate cells and extract fragmented chromatin out of the nuclei. This suspension was centrifuged at 20,000 × g in 10 minutes at 4 °C; the top fraction -T- was collected. Each of the S, T, and B fractions was then treated with 1 mL of 25% trichloroacetic acid (TCA), and DNA precipitated overnight at 4 °C. Precipitated DNA was centrifuged, hydrolyzed with 5% TCA at 90 °C, and stained with freshly prepared DPA reagent -Sigma Chemicals-. Two 200 µL of aliquots in each tube were moved to a 96-well plate after a color development of about 4 hours at 37 °C and "optical density" (OD) was measured at 600 nm with a multiwell spectrophotometer reader (BIOLINE ELISA Reader, 450 nm equivalent). Each fraction was triplicately read. The percentage of fragmented DNA was calculated as:

$$\% \text{ Fragmented DNA} = [(S + T) / (S + T + B)] \times 100$$

2.8. Agarose Gel Electrophoresis

Genomic DNA integrity was independently confirmed by agarose gel electrophoresis. Genomic DNA was isolated from both treated -S/HFB4- and control (C/HFB4) fibroblasts using a saturated NaCl precipitation protocol adapted from Kuo et al. [22]. Cell lysates were combined with 0.4 mL of saturated NaCl solution, incubated on ice for 5 minutes, and centrifuged at 2000 rpm for 30 minutes. Genomic DNA was precipitated with chilled ethanol and recovered by centrifugation. The DNA pellet was resuspended in TAE buffer (40 mM Trisacetate, 1 mM EDTA, pH 8.0) and resolved by electrophoresis on a 1% agarose gel containing 0.5 µg/mL ethidium bromide. DNA bands were visualized under UV

transillumination and documented photographically.

2.9. Surface Characterization of INOX using SEM

Nanoksa G-Plus samples were washed with isopropanol and dried properly to remove surface contaminants and avoid the outgassing of the sample under vacuum conditions. A small representative parts of the material were affixed to conductive aluminum stubs with a double-sided carbon adhesive tape. Since the material is non-conductive, the specimens were sputter coated with a thin film of gold using a sputter coater (S150A, Edwards, England) in order to avoid charging of surfaces in the electron beam as it passes through. A "field-emission scanning electron microscope" (FESEM; QUANTA FEG 250, Thermo Fisher Scientific, FEI, USA) with high-vacuum conditions was used to analyse surface morphology and microstructural features.

2.10. Scanning Electron Microscopy Evaluation of Cell Morphology

The morphological response of fibroblast cells exposed to INOX was evaluated using scanning electron microscopy SEM. HFB4 cells were seeded onto sterile INOX specimens placed in culture plates and incubated under standard culture conditions (37 °C, 5% CO_2) for 24 hours. After incubation, samples were gently washed with "phosphate-buffered saline" (PBS) to remove non-adherent cells and fixed with 2.5% glutaraldehyde for 2 hours at 4 °C.

Following fixation, specimens were dehydrated through a graded ethanol series -30%, 50%, 70%, 90%, and 100%-, air-dried, and mounted onto aluminum stubs using conductive carbon tape. Samples were sputter-coated with a thin gold layer using a sputter coater (S150A, Edwards, England) to enhance conductivity. Cell morphology and attachment characteristics were examined using a "field-emission scanning electron microscope" (FESEM; QUANTA FEG 250, Thermo Fisher Scientific, USA) under high-vacuum conditions. Images were captured at different magnifications to assess cell spreading, adhesion, and cytoplasmic extensions.

2.11. Statistical Analysis

All experiments were performed in triplicate, and data are presented as "mean ± standard deviation" (SD). Statistical analyses were conducted using "GraphPad Prism software" (version 9.0; GraphPad Software Inc., San Diego, CA, USA). Normality of data distribution was assessed using the "Shapiro–Wilk test". For the MTT assay, optical density values of treated cells were normalized to those of untreated controls to determine percentage cell viability. The half-maximal inhibitory concentration (IC_{50}) was estimated using nonlinear regression analysis (MasterPlex 2010 software). Materials exhibiting ≥70% cell viability were classified as non-cytotoxic in accordance with ISO 10993-5 criteria. Relative gene expression for ALP, RUNX2, and OCN was calculated using the comparative $2^{-}\Delta\Delta Ct$ method with GAPDH as the endogenous reference gene. Each RT-qPCR reaction was performed in technical triplicate.DNA fragmentation percentages obtained from the DPA assay were compared between treated and control groups using an unpaired Student's t-test. A p-value < 0.05 was considered statistically significant

3. RESULTS

3.1. Cell Viability (MTT Assay)

The cytotoxic effect of the tested material on HFB4 cells was evaluated using the MTT assay at 570 nm. OD values of treated cells ranged from 0.35 to 0.43 across the tested samples, as shown in Table 1. The corresponding cell viability percentages ranged from 82.62% to 101.59% relative to the untreated control group, which demonstrated a mean OD value of approximately 0.42 and was considered 100% viable. A gradual increase in cell viability was observed across the tested samples, with the lowest viability recorded in Sample 1 (82.62%) and the highest in Sample 12 (101.59%). All tested groups exhibited cell viability values above 70%.

The line graph displays HFB4 cell viability (%) across increasing concentrations or units on a logarithmic scale (x-axis). The x-axis represents the variable in powers of 2, ranging from 2 to 4096, while the y-axis shows cell viability percentage, ranging from 0% to 120%.

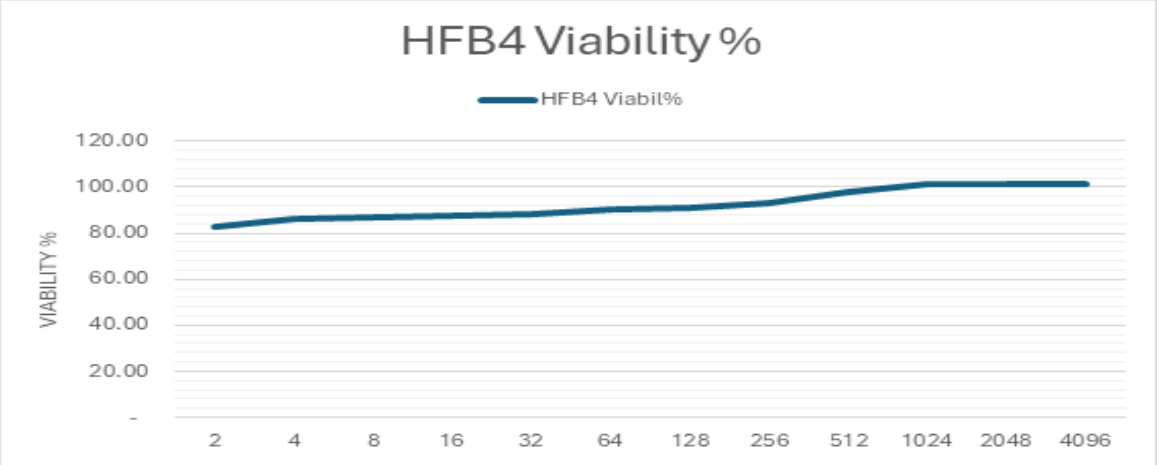

Figure 2: A plotted line diagram presenting the results of the MTT assay.

The plotted line diagram (Figure 2) indicates a gradual increase in cell viability as the x-axis values increase. Initially, at the lower range (2–32), the viability starts around 82–88%. With higher values (64–256), viability rises slowly to approximately 92–94%. Beyond 512, the viability approaches 100%, slightly exceeding it at the highest values (1024–4096), suggesting a minor stimulatory effect at higher concentrations.

Overall, the diagram suggests that HFB4 cells maintain or slightly increase their viability across the tested range, with no evidence of cytotoxicity even at the highest values.

3.2. Osteogenic Gene Expression RT-qPCR

Analysis of RT-qPCR showed that all three osteogenic target genes were significantly upregulated in INOX-treated HFB4 fibroblasts S/HFB4 as compared to untreated controls C/HFB4 Table 2; Figure 3. The strongest differential Ct shift was observed with alkaline phosphatase ALP: the ΔCt ALP GAPDH was 7.81 in control cells and 6.09 in treated cells, with a ΔΔCt of -1.72 and a fold change of 2.96, which indicates that the expression of ALP was increased approximately 3-fold following INOX exposure.

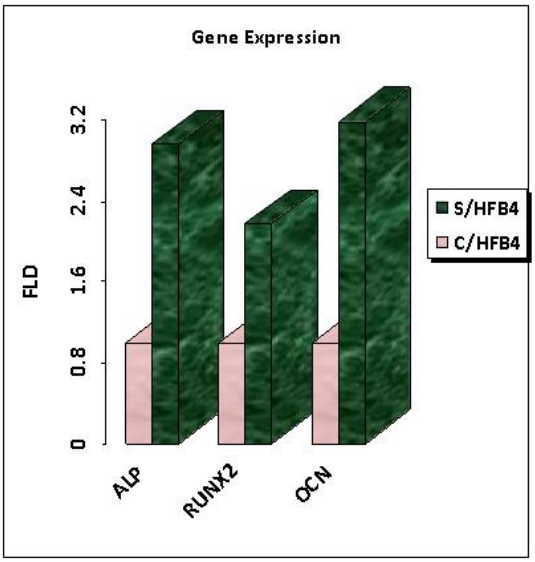

Figure 3: RT-qPCR analysis of osteogenic gene expression in HFB4 cells. Fold changes FLD of ALP, RUNX2, and OCN are shown for S/HFB4 INOX-treated, green versus C/HFB4 control, pink. Treated cells exhibited higher expression of all markers compared to controls.

Table 2: RT-qPCR Analysis results.

	Sample		Gene expression		
	code	cells	Fold Change		
			ALP	RUNX2	OCN
1	S/HFB4	HFB4	2.964	2.175	3.178
2	C/HFB4	---	1.000	1.000	1.000

The expression of RUNX2 was also upregulated, with ΔCt values of 8.73 and 7.50 in the control and treated cells respectively, leading to a ΔΔCt of -1.23 and a fold change of 2.18. The highest relative upregulation was observed with Osteocalcin OCN/BGLAP, with ΔCt values of 12.58 in control cells and 10.80 in INOX-exposed cells, and a ΔΔCt of -1.83 and a fold change of 3.18. Directional upregulation in all three genes was consistent, indicating that an osteogenic transcriptional program is activated by INOX exposure in fibroblasts, but not a cytotoxic stress response.

3.3. DNA Fragmentation Analysis

The DNA integrity was determined by the DPA colorimetric assay in INOX-treated S/HFB4 and control C/HFB4 HFB4 cells. Table 3 shows the results. The DNA fragmentation percentage of the treated group was 2.144 ± 0.08%, whereas the control group was 1.801 ± 0.05%. Despite the treated group showing a marginally higher fragmentation index, the values of both indices are very low absolute numbers of DNA fragmentation that are far lower than apoptosis or other genotoxic damage thresholds.

Table 3: DNA fragmentation levels in HFB4 cells in the DPA assay.

Ser	Sample			DNA fragmentation	SD
	code	cells	IC50	%	
1	**S**	HFB4	---	**2.144**±0.08	
2	**C**	---	---	**1.801**±0.05	

OD values were consistently measured by triplication: T OD values were 0.022, 0.017, and 0.15 at the top and B values were 0.823, 0.819 and 0.822 at the bottom in the treated group. For the control group, T fraction OD values were 0.015, 0.013, and 0.016, with B values of 0.792, 0.802, and 0.806. The fact that the most common OD signal in the B intact chromatin fraction of both groups was that, demonstrates that most of the cellular DNA was still intact after exposure to INOX.

These findings were independently supported by agarose gel electrophoresis. The control and treated cell samples showed bright and high-molecular-weight DNA bands in the upper portion of every gel lane, which is identical to intact genomic DNA. No typical apoptotic DNA laddering pattern, periodic, 180-200 bp fragments were seen in both groups, which ruled out programmatic cell death or any serious genotoxic fragmentation due to INOX exposure.

represent blank readings and ΔT/ΔB represent corrected OD differences used to compute fragmentation.

3.4. Scanning Electron Microscopic evaluation:

3.4.1 Surface Characterization

FESEM analysis of INOX Nanoksa G-Plus samples indicated that the surface microstructure was heterogeneous which is typical of a nano-filled polymer composite. The surface had an irregular micro-scale topography which could be attributed to the distribution of the nano-zirconia and nano-carbon filler particles in the polymer matrix. No apparent surface defects, cracks or delamination were observed. Surface micro-roughness in the submicron range is also interesting biologically since surface topography in this range of nanoscale has been observed to increase protein adsorption and facilitate integrin-mediated cell attachment and spreading.

3.4.2 Scanning Electron Microscopy Evaluation of Cell Morphology:

SEM found that the cellular morphology of HFB4 fibroblasts remained normal after being exposed to INOX. Cells were found to be strongly adherent to surface of the material, and their morphology was that of flattened spindle-like fibroblasts.

Many cytoplasmic extensions and filopodia could be seen projecting out of the cell body towards the material surface indicating active cell adhesion and spreading. No cytotoxic stress morphological characteristics, including cellular shrinkage, membrane blebbing, or detachment were observed.

These results are qualitative and reinforce the cytocompatibility findings of the MTT assay and point to the fact that INOX is a surface environment that supports fibroblasts attachment and growth. Figure 6 illustrates micrographs of SEM.

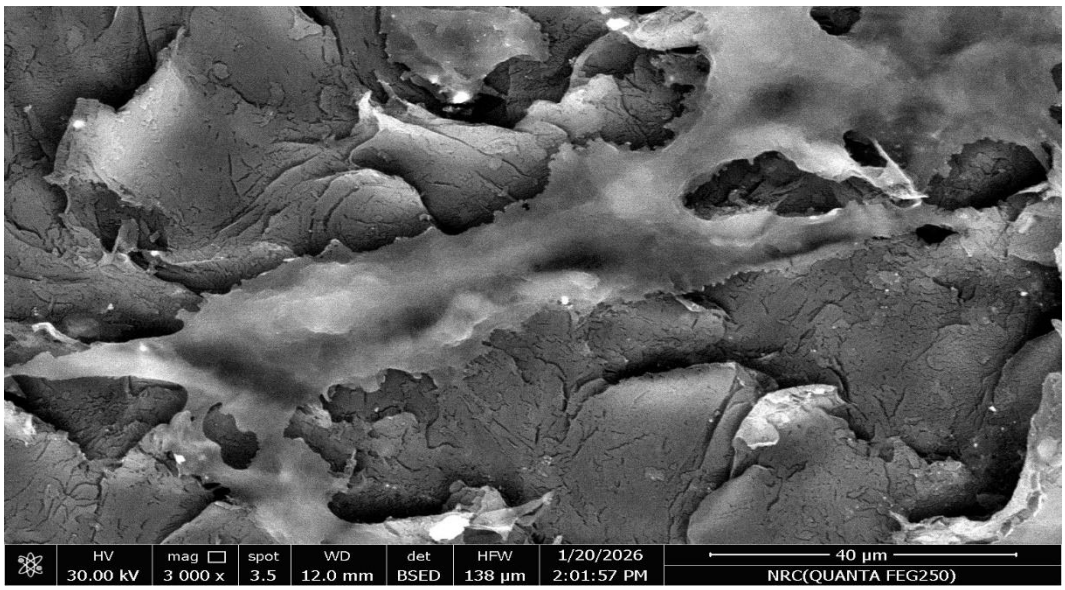

Figure 6: Scanning Electron Microscope photograph showing normal cellular morphology following exposure to INOX.

4. DISCUSSION

An early in vitro biological assessment of INOX Nanoksa G-Plus as a nano-reinforced high-performance polymer is being used as a current prosthetic framework material in the field of implant dentistry and its potential biological activity in a regenerative environment is of interest to the present study. Several supplementary analytical methods were used, such as cytocompatibility testing with the MTT assay, osteogenic gene expression analysis with RT-qPCR, analysis of DNA integrity with the DPA assay and agarose gel electrophoresis, and SEM to describe the material surface and morphology of fibroblasts after exposure to the materials. All these results together indicate that INOX is not only biologically safe but can even positively influence the cellular mechanisms that underlie periodontal and peri-implant tissue regeneration.

An extract-based exposure model was used, in line with ISO 10993-5 and ISO 10993-12 guidelines, which suggest the assessment of the biological impact of the possible leachable chemicals, residual monomers, or degradation products emitted by biomaterials. This technique offers a controlled and reproducible method of initial biocompatibility study prior to direct-contact or three-dimensional scaffold studies. HFB4 human fibroblasts were chosen as a standardized and widely used cell line in biomaterial cytocompatibility as this cell line allows reproducible testing and reduces the variability of the donor with respect to primary cultures. Though periodontal ligament fibroblasts would offer more tissue specificity, they cannot be easily isolated and therefore only freshly extracted teeth can be used and yield limited proliferation and donor dependent variations thus they should be investigated in the future.

The MTT assay showed a positive cytocompatibility profile of INOX since cell viability was above the ISO 10993-5 non-cytotoxicity limit at all the tested extract concentrations. The fact that the IC50 is not measurable in the test range also indicates the low cytotoxic potential of the material during the experiment. These results are in line with the literature assessing polymer scaffolds in the context of implant dentistry, such as 3D-printed or milled PEEK scaffolds, which have also shown a high degree of fibroblast and osteoblast viability and are generally considered to have a good biocompatibility [23,24]. The observed small rise in viability at more extreme dilutions, where values are nearly or slightly surpassing 100% is probably attributable to normalization of cellular metabolic activity as extract concentrations drop below biologically relevant limits and not to a real proliferative effect.

Biomarkers of gene expression are common to assess early cellular responses to biomaterials and to give an indication of their ability to induce regenerative pathways [25]. The exposure of INOX in the current research was linked to elevated levels of the major osteogenic markers, such as ALP, RUNX2, and OCN, which is an indication of transcriptional pathways that have been triggered by the exposure to INOX. ALP is generally considered to be an early marker of osteogenic commitment related to mineralization processes [26], whereas RUNX2 is a key transcription factor that controls the differentiation of osteoblasts and cementoblasts [27]. OCN is a subsequent osteogenic maturation marker, indicating maturation toward a mineralizing type [28]. These are in line with earlier reports that reveal that osteogenic markers are upregulated in fibroblasts and other mesenchymal cells after exposure to bioactive composite scaffolds [29] and PEEK scaffolds [30].

The concurrent upregulation of early, intermediate, and late osteogenic markers suggests that INOX may promote a coordinated osteogenic transcriptional response rather than a nonspecific cellular stress reaction. Similar expression patterns have been reported in response to bioactive materials such as calcium silicate cements, bioglass, and nanohydroxyapatite scaffolds, which are known to stimulate osteogenic differentiation in fibroblasts and periodontal progenitor cells through surface chemistry and physicochemical cues [23,30]. The nano-zirconia and nano-carbon filler components of INOX may contribute to this response through mechanisms such as modulation of the local ionic microenvironment and surface roughness–mediated mechanotransduction. In addition, carbon-based nanomaterials have been reported to influence cellular signaling pathways, including reactive oxygen species–related pathways involved in differentiation processes [31], although further studies are required to confirm these mechanisms in relation to INOX. According to a recent systematic review, from a periodontal regeneration perspective, the observed osteogenic gene expression profile in fibroblasts is of direct translational relevance.[32].

Periodontal ligament fibroblasts are a heterogeneous population that includes progenitor subpopulations capable of differentiating into cementoblasts, osteoblasts, and PDL fibroblasts proper, depending on the microenvironmental signals they receive [32]. An ideal scaffold to use in “guided tissue regeneration” (GTR) and “guided bone regeneration” (GBR) would be one that can induce osteogenic transcription in PDL-associated cells, but not induce cytotoxicity [33]. This is especially compelling by the fact that the INOX is capable of upregulating RUNX2, OCN, and ALP, the transcriptional gateway to osteoblast and cementoblast lineage commitment.

The results of the DNA integrity, as found in the DPA assay and agarose gel electrophoresis give one more piece of evidence of the safety of the tested material. Despite some increase in the degree of DNA fragmentation in INOX-treated cells over the controls, the difference was statistically insignificant, and fell within the range of normal cellular turnover in an organism, as opposed to genotoxic damage. These results are similar to other researchers who have tested polymer-based biomaterials in implant dentistry and even exhibit low levels of DNA fragmentation and no genotoxic effects in fibroblast and osteoblastic cell models [34].

SEM analysis was another step that gained better

understanding of the surface and cellular interactions related to INOX. The observed heterogeneous microstructure with FESEM is probably due to nano-filled composite structure of the material, where the nano-zirconia and nano-carbon fillers are dispersed in the polymer matrix, creating micro- and submicron-scale surface roughness, which can promote protein adsorption and integrin-mediated cell adhesion. In line with this observation, the fibroblasts cultured on INOX had a characteristic spindle-shaped morphology with observable cytoplasmic extensions and filopodia indicating that the cells were actively attaching to the material surface and spreading. The lack of the morphological features usually related to cytotoxic stress only contributes to the positive cytocompatibility profile achieved in the viability tests. Fibroblasts have been shown to exhibit similar cellular morphology on polymer-based biomaterials in implant dentistry, such as PEEK-based frameworks, and surface microtopography has been indicated to have a role in mediating cell adhesion and cytoskeletal organization [35].

The current study has several shortcomings that need to be mentioned. The cell line used is a validated, standardized model of cell types commonly used in cytotoxicity and gene expression studies but may not accurately recapitulate the biological behavior of periodontal ligament or gingival fibroblasts that have specific progenitor properties and may behave differently to osteogenic stimuli. This cell line was mostly used because of the scarcity of primary periodontal cells that were available in the experimental condition. The findings should be thus validated in the future by using periodontal ligament fibroblasts, gingival fibroblasts and osteoblastic cell lines to more effectively capture a cellular environment of periodontal tissues. Moreover, the experiment employed an extract-based exposure model, suitable to standardized biocompatibility evaluation but not entirely representative of direct cell-material interactions at a scaffold interface. Keeping this in mind, it is worthwhile to conduct further studies with direct-contact models and three-dimensional culture systems in order to simulate the conditions in vivo more accurately.

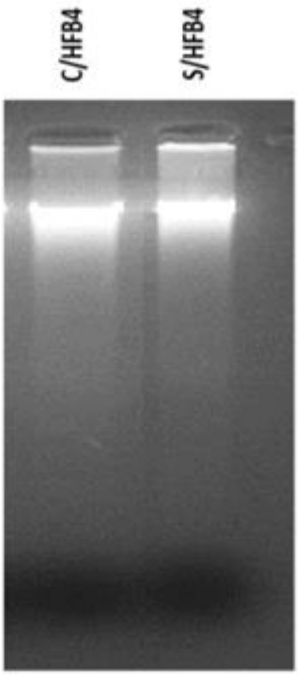

Figure 4: DNA integrity of HFB4 cells assessed by agarose gel electrophoresis

Nevertheless, even with these drawbacks, the current results present initial biological information on the potential of INOX as a regenerative biomaterial. The demonstrated cytocompatibility, response of osteogenic genes expression and maintenance of DNA integrity could be an indication that the material can have characteristics that can make it useful in cellular compatibility and regeneration. The observations may be especially topical in light of the mechanical stability and the CAD/CAM processability, which has already been reported with the help of the similar polymer-based materials utilized in the sphere of prosthetic dentistry. However, more studies are needed to further define its biological performance. Future research can address the surface modification approaches including

plasma treatment or bioactive surfaces and the development of three-dimensional scaffold structures and in vivo analysis in periodontal or peri-implant defect models.

5. CONCLUSION

In the constraints of this in vitro study, INOX had a positive biological response, showing high cell viability, low levels of DNA fragmentation, and amplified expression of osteogenic indicators in fibroblasts. Observations of SEM also indicated that the material surface could have cellular attachment and spreading. These results, combined, suggest that INOX is cytocompatible and can stimulate

osteogenic differentiation-related cellular reactions.

Based on its mechanical properties and CAD/CAM processability, INOX could be a future candidate material to develop as a biomaterial in regenerative applications. However, additional research, which involves periodontal cell types, models of direct contact, and experimental systems in vivo, is needed to describe its regenerative prospectivity further.

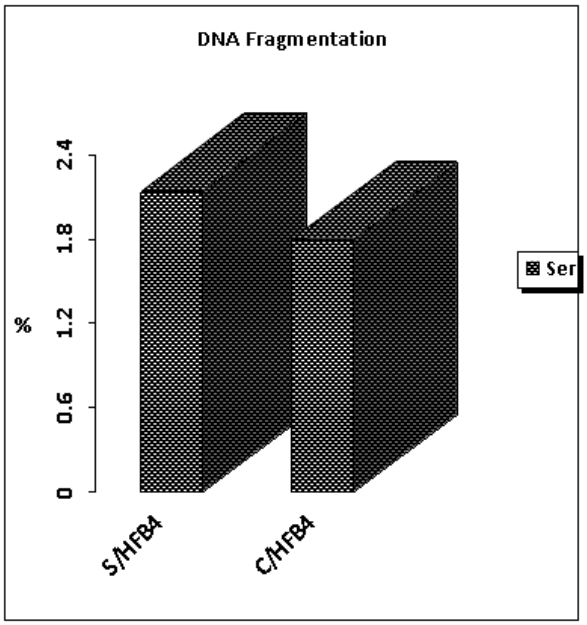

Figure 5: Comparative analysis of DNA fragmentation % in treated S/HFB4 and untreated control C/HFB4 cells, demonstrating increased fragmentation in the test group.

Author Contributions

Conceptualization, G.A.; Methodology, M.E, H.E; Formal analysis, M.E; Investigation, G.A, M.I, M.E; Resources, H.E.; Data curation, M.I.; Writing, original draft preparation, M.I.; Writing, review and editing, G.A, M.E.; Supervision, G.A.; All authors have read and agreed to the published version of the manuscript.

Funding

This research received no external funding.

Institutional Review Board Statement

The study was conducted in accordance with the Declaration of Helsinki and approved by the Research Ethics Committee of the Faculty of Dentistry, Cairo University, Approval No. 10-25. No human subjects or animal experiments were involved in this study. Clinical trial registry number NCT07381153.

Informed Consent Statement

Not applicable. This study used commercially sourced human cell lines and did not involve the collection of samples from human participants.

Data Availability Statement

The datasets generated and analyzed during the current study are available from the corresponding author upon reasonable request.

Conflicts of Interest

The authors declare no conflict of interest.

REFERENCES

1. Saleh, M.H.; Dias, D.R.; Kumar, P. The economic and societal impact of periodontal and peri-implant diseases. Periodontology 2000 2025, 98, 100-118.
2. Tonetti, M.S.; Greenwell, H.; Kornman, K.S. Staging and grading of periodontitis: Framework and proposal of a new classification and case definition. Journal of periodontology 2018, 89, S159-S172.
3. Fragkioudakis, I.; Tseleki, G.; Doufexi, A.-E.; Sakellari, D. Current concepts on the pathogenesis of peri-implantitis: a narrative review. European journal of dentistry 2021, 15, 379-387.
4. Ansari, M. Bone tissue regeneration: biology, strategies and interface studies. Progress in biomaterials 2019, 8, 223-237.
5. Saberian, E.; Jenča, A.; Zafari, Y.; Petrášová, A.; Zare-Zardini, H.; Jenčová, J. Scaffold application for bone regeneration with stem cells in dentistry: literature review. Cells 2024, 13, 1065.
6. Xing, F.; Li, L.; Zhou, C.; Long, C.; Wu, L.; Lei, H.; Kong, Q.; Fan, Y.; Xiang, Z.; Zhang, X. Regulation and directing stem cell fate by tissue

engineering functional microenvironments: scaffold physical and chemical cues. Stem cells international 2019, 2019, 2180925.

7. Chen, H.; Song, G.; Xu, T.; Meng, C.; Zhang, Y.; Xin, T.; Yu, T.; Lin, Y.; Han, B. Biomaterial scaffolds for periodontal tissue engineering. Journal of Functional Biomaterials 2024, 15, 233.
8. Top, N.; Şahin, İ.; Gökçe, H.; Gökçe, H. Computer-aided design and additive manufacturing of bone scaffolds for tissue engineering: state of the art. Journal of Materials Research 2021, 36, 3725-3745.
9. Bathala, L.; Majeti, V.; Rachuri, N.; Singh, N.; Gedela, S. The role of polyether ether ketone (PEEK) in dentistry–a review. Journal of medicine and life 2019, 12, 5.
10. Benakatti, V.B.; Sajjanar, J.A.; Acharya, A. Polyetheretherketone (PEEK) in dentistry. J Clin Diagn Res 2019, 13.
11. Alqutaibi, A.Y.; Alghauli, M.A.; Algabri, R.S.; Hamadallah, H.H.; Aboalrejal, A.N.; Zafar, M.S.; Fareed, M.A. Applications, modifications, and manufacturing of polyetheretherketone (PEEK) in dental implantology: A comprehensive critical review. International Materials Reviews 2025, 70, 103-136.
12. Moharil, S.; Reche, A.; Durge, K.; Moharil, S.S. Polyetheretherketone (PEEK) as a biomaterial: an overview. Cureus 2023, 15.
13. Abdelrahim, R.A.; Ezzeldine, A.A.; Abdellah, M.; Elghazawi, S.S. Effect of thermal ageing on flexural strength and microhardness of novel High-Performance polymer (Nanoksa G-Plus) in comparison to a widely used Bio-HPP/PEEK. Dentistry Journal 2025, 13, 370.
14. Omar, S.; Elshenawy, E.A.; Elsharkawy, S.M. Comparison of marginal gap in implant-supported hybrid nanoceramic crowns fabricated by additive vs. subtractive manufacturing. BMC Oral Health 2026.
15. Suarez-Lopez del Amo, F.; Monje, A.; Padial-Molina, M.; Tang, Z.; Wang, H.-L. Biologic agents for periodontal regeneration and implant site development. BioMed research international 2015, 2015, 957518.
16. Hosoya, A.; Shalehin, N.; Takebe, H.; Fujii, S.; Seki, Y.; Mizoguchi, T.; Shimo, T.; Iijima, M.; Irie, K. Stem cell properties of Gli1-positive cells in the periodontal ligament. Journal of Oral Biosciences 2020, 62, 299-305.
17. Han, J.; Leeuwenburgh, S.C.; Jansen, J.A.; Yang, F.; van Oirschot, B.A. Biological processes in gingival tissue integration around dental implants. Tissue Engineering Part B: Reviews 2025, 31, 1-19.
18. Tavelli, L.; McGuire, M.K.; Zucchelli, G.; Rasperini, G.; Feinberg, S.E.; Wang, H.L.; Giannobile, W.V. Extracellular matrix-based scaffolding technologies for periodontal and peri-implant soft tissue regeneration. Journal of periodontology 2020, 91, 1725.
19. Thangaraju, P.; Varthya, S.B. ISO 10993: biological evaluation of medical devices. In Medical device guidelines and regulations handbook; Springer: 2022; pp. 163-187.
20. Heise, T.; Sawyer, A.Y.; Hirai, T.; Schaible, S.; Sy, H.; Wickramasekara, S. Report on investigation of ISO 10993–12 extraction conditions. Regulatory Toxicology and Pharmacology 2022, 131, 105164.
21. Bandgar, S.S.; Yadav, H.M.; Shirguppikar, S.S.; Shinde, M.A.; Shejawal, R.V.; Kolekar, T.V.; Bamane, S.R.; Sneha, S.B.; Hemraj, M.Y.; Shailesh, S.S. Enhanced hemolytic biocompatibility of hydroxyapatite by chromium (Cr 3+) doping in hydroxyapatite nanoparticles synthesized by solution combustion method. Journal of the Korean Ceramic Society 2017, 54, 158-166.
22. Kuo, J.-h.S.; Jan, M.-s.; Jeng, J.; Chiu, H.W. Induction of apoptosis in macrophages by air oxidation of dioleoylphosphatidylglycerol. Journal of controlled release 2005, 108, 442-452.
23. Peng, T.-Y.; Shih, Y.-H.; Hsia, S.-M.; Wang, T.-H.; Li, P.-J.; Lin, D.-J.; Sun, K.-T.; Chiu, K.-C.; Shieh, T.-M. In vitro assessment of the cell metabolic activity, cytotoxicity, cell attachment, and inflammatory reaction of human oral fibroblasts on polyetheretherketone (PEEK) implant–abutment. Polymers 2021, 13, 2995.
24. Brum, R.S.; Monich, P.R.; Berti, F.; Fredel, M.C.; Porto, L.M.; Benfatti, C.A.; Souza, J.C. On the sulphonated PEEK for implant dentistry: Biological and physicochemical assessment. Materials Chemistry and Physics 2019, 223, 542-547.
25. Gaharwar, A.K.; Singh, I.; Khademhosseini, A. Engineered biomaterials for in situ tissue regeneration. Nature Reviews Materials 2020, 5, 686-705.
26. Golub, E.E.; Boesze-Battaglia, K. The role of alkaline phosphatase in mineralization. Current opinion in Orthopaedics 2007, 18, 444-448.
27. Franceschi, R.T.; Xiao, G. Regulation of the osteoblast-specific transcription factor, Runx2: Responsiveness to multiple signal transduction pathways. Journal of cellular biochemistry 2003, 88, 446-454.
28. Dao, D.Y.; Jonason, J.H.; Zhang, Y.; Hsu, W.; Chen, D.; Hilton, M.J.; O'Keefe, R.J. Cartilage-specific β-catenin signaling regulates chondrocyte maturation, generation of ossification centers, and perichondrial bone formation during skeletal development. Journal of Bone and Mineral Research 2012, 27, 1680-1694.
29. Polini, A.; Pisignano, D.; Parodi, M.; Quarto, R.; Scaglione, S. Osteoinduction of human mesenchymal stem cells by bioactive composite scaffolds without supplemental osteogenic growth factors. PloS one 2011, 6, e26211.
30. Ragni, E.; Perucca Orfei, C.; Bidossi, A.; De Vecchi, E.; Francaviglia, N.; Romano, A.;

Maestretti, G.; Tartara, F.; de Girolamo, L. Superior osteo-inductive and osteo-conductive properties of trabecular titanium vs. PEEK scaffolds on human mesenchymal stem cells: a proof of concept for the use of fusion cages. International journal of molecular sciences 2021, 22, 2379.

31. Yuan, X.; Zhang, X.; Sun, L.; Wei, Y.; Wei, X. Cellular toxicity and immunological effects of carbon-based nanomaterials. Particle and fibre toxicology 2019, 16, 18.
32. Li, M.; Zhang, C.; Yang, Y. Effects of mechanical forces on osteogenesis and osteoclastogenesis in human periodontal ligament fibroblasts: A systematic review of in vitro studies. Bone & joint research 2019, 8, 19-31.
33. Yamada, S.; Shanbhag, S.; Mustafa, K. Lesko, L.; Jungova, P.; Culenova, M.; Thurzo, A.; Danisovic, L. Polymer-Based Scaffolds as an Implantable Material in Regenerative Dentistry: A Review. Journal of Functional Biomaterials 2025, 16, 80.
34. Pidhatika, B.; Widyaya, V.T.; Nalam, P.C.; Swasono, Y.A.; Ardhani, R. Surface Modifications of High-Performance Polymer Polyetheretherketone (PEEK) to Improve Its Biological Performance in Dentistry. Polymers 2022, 14, 5526.